

## Article

# Removal of Chloroacetanilide Herbicides from Water Using Heterogeneous Photocatalysis with TiO<sub>2</sub>/UV-A

Nikola Roulová<sup>1</sup>, Kateřina Hrdá<sup>2</sup>, Michal Kašpar<sup>3</sup>, Petra Peroutková<sup>2</sup>, Dominika Josefová<sup>2</sup> and Jiří Palarčík<sup>2,\*</sup>

<sup>1</sup> Department of Biological and Biochemical Sciences, University of Pardubice, Studentská 573, 532 10 Pardubice, Czech Republic; nikola.roulova@student.upce.cz

<sup>2</sup> Institute of Environmental and Chemical Engineering, University of Pardubice, Studentská 573, 532 10 Pardubice, Czech Republic; katerina.hrda@upce.cz (K.H.); petra.peroutkova@upce.cz (P.P.); dominika.josefova@student.upce.cz (D.J.)

<sup>3</sup> Department of Analytical Chemistry, University of Pardubice, Studentská 573, 532 10 Pardubice, Czech Republic; michal.kaspar3@student.upce.cz

\* Correspondence: jiri.palarcik@upce.cz

**Abstract:** Chloroacetanilide herbicides are widely used in the agricultural sector throughout the world. Because of their poor biodegradability, high water solubility, and long persistence, chloroacetanilide herbicides have a high potential to contaminate water, and conventional water treatment processes do not ensure sufficient removal. Therefore, heterogeneous photocatalysis using TiO<sub>2</sub>/UV-A was investigated for the degradation of alachlor, acetochlor, and metolachlor from water. Two commercially available TiO<sub>2</sub> (P25 and AV-01) were used as photocatalysts. Different experimental setups were also tested. In addition, the toxicity of single herbicides and mixtures of their photocatalytic degradation products to the freshwater alga *Chlorella kessleri* was investigated via a growth inhibition test. The maximum removal efficiency for alachlor, acetochlor, and metolachlor was 97.5%, 93.1%, and 98.2%, respectively. No significant differences in the removal efficiency of chloroacetanilide herbicides were observed for the photocatalysts used. Although the concentrations of all herbicides during photocatalysis decreased, the toxicity of the resulting mixtures of degradation products increased or remained the same, indicating the formation of toxic degradation products.

**Keywords:** algal growth inhibition test; *Chlorella kessleri*; chloroacetanilide herbicides; heterogeneous photocatalysis; photocatalytic degradation; titanium dioxide; UV-A LED



**Citation:** Roulová, N.; Hrdá, K.; Kašpar, M.; Peroutková, P.; Josefová, D.; Palarčík, J. Removal of Chloroacetanilide Herbicides from Water Using Heterogeneous Photocatalysis with TiO<sub>2</sub>/UV-A. *Catalysts* **2022**, *12*, 597. <https://doi.org/10.3390/catal12060597>

Academic Editor: Antonio Eduardo Palomares

Received: 30 April 2022

Accepted: 26 May 2022

Published: 30 May 2022

**Publisher's Note:** MDPI stays neutral with regard to jurisdictional claims in published maps and institutional affiliations.



**Copyright:** © 2022 by the authors. Licensee MDPI, Basel, Switzerland. This article is an open access article distributed under the terms and conditions of the Creative Commons Attribution (CC BY) license (<https://creativecommons.org/licenses/by/4.0/>).

## 1. Introduction

Herbicides are an integral part of modern agricultural practices, and are used intensively to prevent, destroy, or mitigate undesirable vegetation, and their use has been increasing continuously over the past decades [1–3]. Unfortunately, the benefits generated by their use are accompanied by several negative effects on human health and the environment [4,5]. The extensive use of herbicides leads to soil and water contamination that is primarily due to agricultural runoff [2,3]. The presence of herbicides in aquatic ecosystems is concerning, as they can affect several levels of biological organization, from the molecular to the ecosystem level [6].

Systematic and selective chloroacetanilide herbicides represent one of the major classes of herbicides that are applied worldwide in the agricultural sector to control broadleaf weeds and annual grasses for crops such as corn, soybeans, sorghum, cotton, sugar beet, or sunflower [1,7,8]. Chloroacetanilides are mainly the *N*-alkoxyalkyl-*N*-chloroacetyl-substituted derivatives of aniline [1]. The mode of action of chloroacetanilide herbicides consists of inhibiting the early development of susceptible weeds by preventing the synthesis of alkyl chains longer than C18 outside the chloroplast, thus affecting the elongation of

very-long-chain fatty acids, which are important factors in the plasma membrane and cell expansion [7,9–12].

Acetochlor, metolachlor, and alachlor are among the most commonly used chloroacetanilide herbicides [11]. Due to their relatively high-water solubility, poor biodegradability, low sorption, long environmental persistence, and prolonged half-life, they have a high potential to contaminate water [1,3,13,14]. Therefore, chloroacetanilide herbicides, as well as their metabolites, such as ethane sulfonic acids (ESA) and oxanilic acids (OA), are often detected in ground and surface water. The concentration of the parent compounds varied according to the matrices from 0.1 to 10 µg/L [1,7,8,11]. However, if the water source is strongly influenced by agricultural activities, chloroacetanilide herbicides can reach a concentration of the order of 100 µg/L [15]. Chloroacetanilides have also been detected in drinking water [7]. In addition, herbicides constitute one of the main products of the agrochemical industry found in wastewater [16].

Concern about the influence of chloroacetanilide herbicides on human health and ecosystems has increased in recent years due to the high rate of their use. The main risks represent their high toxicity even at low concentrations, and their almost non-biodegradable nature [2,16]. Metolachlor is classified as a possible human carcinogen, and acetochlor is classified as suggestive evidence of carcinogenic potential [8].

In addition, the removal of chloroacetanilide herbicides from contaminated water is difficult. These compounds negatively impact the activity of microorganisms in activated sludge, indicating that conventional bioremediation-based biological water treatment processes are not suitable for the removal of herbicides [13,16–18]. Furthermore, many conventional physicochemical water treatment processes, such as peroxidation by permanganate, coagulation, filtration, adsorption, and chlorination, do not ensure the removal of herbicides from water [11,13,17]. Therefore, the successful elimination of herbicides in an aqueous environment requires the application of innovative technologies. In this context, advanced oxidation processes (AOPs) represent a particularly effective water treatment technology for the degradation of pesticides, as well as other non-easily removable organic compounds retained in water [4,16]. In general, AOPs use strong oxidation agents, such as hydroxyl radicals (OH•), generated by specific chemical reactions in aqueous solutions, capable of degrading recalcitrant organic pollutants into simple and non-toxic molecules [16,19]. AOPs have acquired high relevance in the field of water treatment mainly due to their high removal efficiency derived from the high reactivity and low selectivity of hydroxyl radicals [20,21]. AOPs are capable of degrading nearly all types of organic contaminants into compounds, with a reduced impact on the environment [22,23]. Furthermore, unlike conventional chemical and biological processes, AOPs represent completely environmentally friendly technology, as they neither transfer pollutants from one phase to another (such as in chemical precipitation and adsorption) nor produce hazardous sludge [23]. AOPs are classified according to the different ways used to produce oxidation agents [19].

Among AOPs, heterogeneous photocatalysis, which uses ultraviolet light ( $\lambda < 400$  nm) as an energy source and an appropriate semiconductor as a photocatalyst, constitutes one of the most distinctive, promising, and effective solutions for the purification of water contaminated with persistent and recalcitrant contaminants [16,17,24–26]. The light absorption by a suitable photocatalyst results in the generation of electrons ( $e^-$ ) with high reducing ability in the conduction band (CB), and holes ( $h^+$ ) with high oxidizing ability in the valence band (VB). VB holes ( $h^+$ ) migrate to the surface of the photocatalyst, where they react with water and hydroxide ions to form hydroxide radicals (OH•), which are the primary oxidant in the photocatalytic oxidation of organic compounds [19,27]. The degradation of alachlor in aqueous solutions using different heterogeneous photocatalytic systems is relatively well-described in the literature [28–35]. On the other hand, less attention is paid to metolachlor and acetochlor, and their photocatalytic degradation has rarely been investigated [36–39].

In addition to photocatalytic oxidation, other AOPs and their combination have been studied for the removal of chloroacetanilide herbicides from water, with alachlor again receiving the most attention. The application of different ozone-based AOPs [40–42], photo-Fenton oxidation [35,43], and electro-oxidation processes [18,44], as well as relatively new plasma-based AOPs, has been reported for the elimination of alachlor in water [45,46]. Metolachlor and acetochlor have been removed by direct ozonation and catalytic ozonation [11,47–49], and the photo-Fenton process [50,51]. Furthermore, electrochemical AOPs have been used for metolachlor degradation [4,52].

Among the semiconductors used as photocatalysts for heterogeneous photocatalysis, titanium dioxide ( $\text{TiO}_2$ ) is the most common because it is distinctive with a large surface area; a good particle size distribution; excellent chemical, thermal, and photochemical stability; and excellent photocatalytic performance. Other benefits of  $\text{TiO}_2$  include relatively low cost, non-toxicity, and no secondary pollution [13,19,25–27].  $\text{TiO}_2$  forms three naturally occurring polymorphic crystalline modifications. Anatase and rutile, with a tetragonal crystal lattice, are the most common forms. Anatase is more efficient than rutile in photocatalysis applications, and shows higher photocatalytic activity. As a result,  $\text{TiO}_2$  photocatalysts generally have a high share of anatase. Nevertheless, the rutile phase is generally considered the most stable phase among all forms of titania. Brookite is the third crystalline form with a rhombic crystal lattice, and, in powder or thin-film forms, shows good stability and even better photocatalytic activity than anatase  $\text{TiO}_2$  [24,53–55]. Commercial  $\text{TiO}_2$  powder, such as crystalline anatase and combinations of anatase and rutile, have been the photocatalysts used the most extensively in the photocatalysis treatment processes [24]. Although  $\text{TiO}_2$  powder (particle size in the range of tens of nanometers) exhibits high effectiveness, it has been established that  $\text{TiO}_2$  in the form of nanoparticles is much more effective as a photocatalyst [21,56]. The better photocatalytic performance of  $\text{TiO}_2$  nanoparticles is derived from the fact that photocatalytic reactions take place on the surface of the photocatalyst, and particles of smaller sizes tend to provide more reactive sites [57]. Generally,  $\text{TiO}_2$  is prepared in the form of powders, crystals, thin films, nanotubes, and nanorods [56].

However, the commercial application of pure  $\text{TiO}_2$  as a photocatalyst is still limited. The biggest obstacles are the relatively low quantum efficiency of pure  $\text{TiO}_2$ , and a considerable reduction in photocatalytic activity by electron-hole recombination [27,58]. Furthermore,  $\text{TiO}_2$  particles are active only under UV light, as they cannot absorb light with wavelengths greater than 398 nm (which comprise only 5% of the sunlight) due to their relatively large bandgap. Thus, the poor photosensitivity of  $\text{TiO}_2$  under visible/solar irradiation is also a problem [21,25,55,58,59]. From this point of view, many concepts are available to improve the photocatalytic properties of  $\text{TiO}_2$  under visible irradiation, such as immobilization of  $\text{TiO}_2$  on different supports, surface modification with organic molecules, doping with metal and non-metal ions, hybridization with carbonaceous nanomaterials, and the addition of oxidants, among others [21,55,57–59].

The environmental applications of  $\text{TiO}_2$ -based heterogeneous photocatalysis in the field of wastewater and water treatment are numerous and include the removal of traditional and emerging pollutants. In addition to chloroacetanilide herbicides, degradation of different classes of herbicides used in the agricultural sector over  $\text{TiO}_2$ -based photocatalysts has also been reported. Heterogeneous photocatalysis was used to remove herbicide diuron [60], atrazine [61], bentazon [62], and terbutylazine [63], among others. In addition, other agrochemicals, such as fungicides [64] and insecticides [65], were degraded by  $\text{TiO}_2$ -based photocatalysis. Considerable attention has been paid to the application of heterogeneous photocatalysis to remove pharmaceuticals from water and wastewater. Photocatalytic degradation of paracetamol [66], diclofenac [67], or ibuprofen [68] has been reported. The emphasis is on the removal of commonly used antibiotics, such as ciprofloxacin [69], ofloxacin [70], sulfamethoxazole-trimethoprim [71], and tetracycline [72].  $\text{TiO}_2$  photocatalysis under ultraviolet light was also used to remove antibiotic-resistant bacteria and antibiotic-resistant genes [73].

Heterogeneous photocatalysis with TiO<sub>2</sub> has been extensively examined for the removal of substances such as phenol [74]. Attention is also paid to the degradation of persistent organic pollutants such as perfluorooctanoic acid [75]. The application in the removal of dyes, such as rhodamine B, methylene blue, and methyl orange, has also been studied [76,77]. TiO<sub>2</sub>/UV photocatalysis was even applied to remove polystyrene nanoparticles [78].

An important property of AOPs is the detoxification of purified water, due to their ability to degrade highly toxic organic compounds into less toxic or non-toxic products [79]. However, in some cases, the oxidation of the parent compound can lead to transformation products or intermediates with similar or even greater toxicity [79,80]. The structural transformation of chemical compounds by AOPs leads to a potential contaminant with new chemical toxicity [80]. For this reason, acute toxicity tests are used during different stages of treatment, which helps to demonstrate the utility of AOPs in reducing the toxicity of contaminated water [79].

Algae are the primary producers and the first level of the aquatic food chain. Therefore, any effect on algae will influence higher trophic levels. Although herbicides were generally designed to be toxic only to particular groups of organisms, nowadays there is undeniable evidence that herbicides, including chloroacetanilides, are not specific to their main target (weeds). As a result, chloroacetanilide herbicides can have considerable adverse effects on other aquatic non-target organisms and, in particular, on algae due to their similarity to plants, since both have the photosynthetic capacity [3,5,6,81].

In view of this fact, the freshwater alga *Chlorella kessleri* was chosen as a test organism for the evaluation of the toxicity of chloroacetanilide herbicides and the mixtures of their degradation products formed during heterogeneous photocatalysis. Species of the *Chlorella* genus (*Chlorophyceae*) are widespread throughout the world and can be found in a variety of aquatic environments, where they represent primary producers, contribute to the self-purification of water, and have many other important ecological functions. *Chlorella kessleri* is a unicellular microalga and is often used in toxicity studies, as it has a short life cycle, can be easily cultured in the laboratory, and many studies have shown that it is sensitive to xenobiotics [82–85].

In summary, this study focuses on the use of heterogeneous photocatalysis with TiO<sub>2</sub>/UV-A for the degradation of the chloroacetanilide herbicides alachlor, acetochlor, and metolachlor. To the best of our knowledge, data on the titania-mediated photocatalyzed transformation of chloroacetanilide herbicides are scarce. Therefore, the main objective of the present study was to design and verify a suitable procedure for the effective elimination of selected chloroacetanilide herbicides from contaminated water using TiO<sub>2</sub>/UV photocatalysis. For this purpose, two commercial titanium dioxide AEROXIDE<sup>®</sup> TiO<sub>2</sub> P25 and PRETIOX<sup>®</sup> TiO<sub>2</sub> AV-01 (hereafter referred to as P25 and AV-01) and different experimental setups were compared. The efficiency of treatment was evaluated for not only herbicide degradation, but also toxicity, in different stages of treatment.

## 2. Results

### 2.1. Photocatalytic Degradation of Alachlor, Acetochlor, and Metolachlor

The photocatalytic degradation of the chloroacetanilide herbicides alachlor, acetochlor, and metolachlor was repeated three times under each experimental condition, and the reported data are the average values obtained from this series of measurements. Figure 1 presents variations in the concentrations of alachlor, acetochlor, and metolachlor during the different experimental setups of the photocatalysis process.

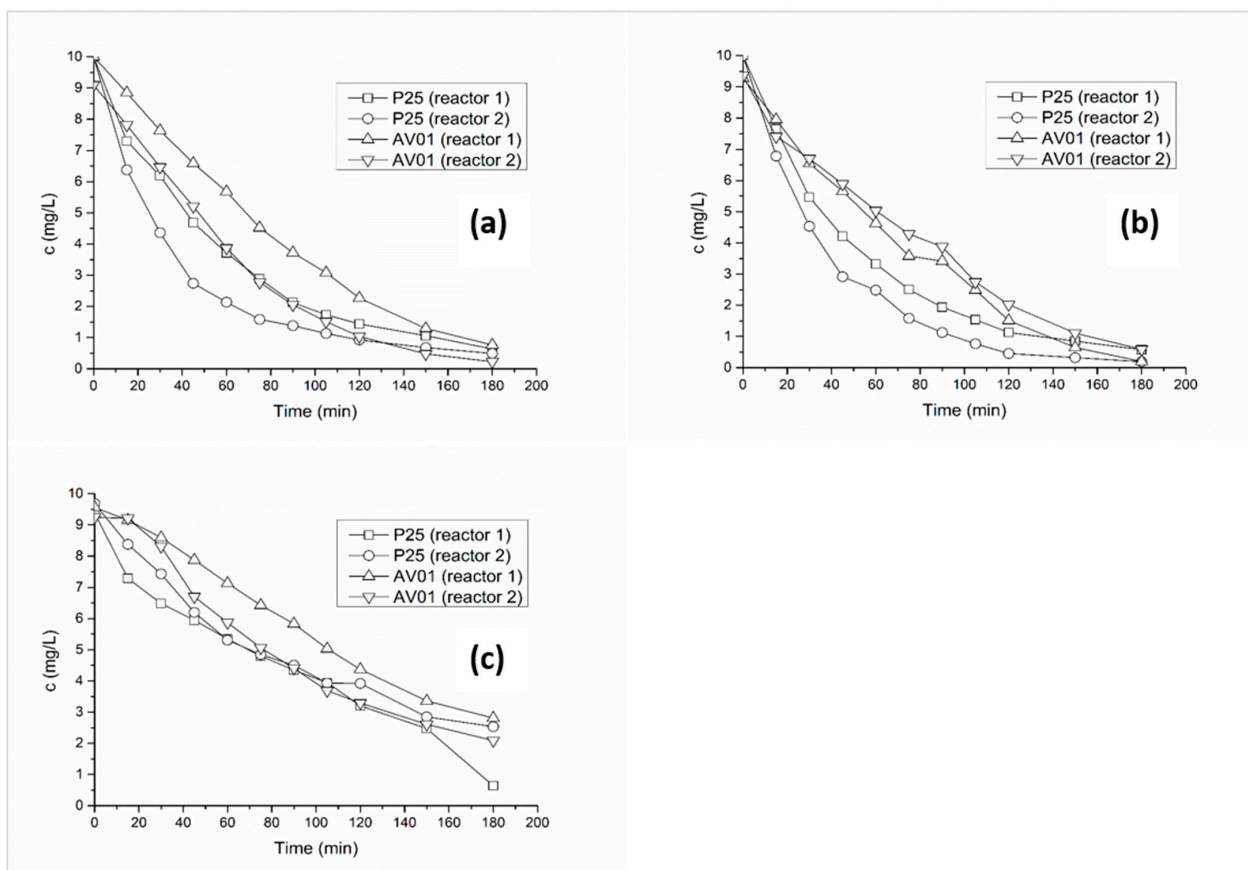


**Figure 1.** Variations in the concentration of herbicides during the different experimental setups of the photocatalysis process: (a) alachlor, (b) metolachlor, (c) acetochlor. The error bars are not included in the graphs, as the measurement error was less than 5% for all measurements. As a result, the error bars are short and smaller than the size of the markers in the plot. Adding error lines would make the graphs confusing.

The highest alachlor removal (97.5%) was achieved using the AV-01 photocatalyst and reactor R2. On the contrary, the combination of photocatalyst AV-01 with reactor R1 showed a removal level of 92.4%, which corresponds to the lowest efficiency for alachlor degradation. The combination of photocatalyst P25 with reactors R1 and R2 resulted in removal levels of 93.9% and 95.1%, respectively, in 180 min. For both photocatalysts, reactor R1 showed a slower degradation profile.

The highest removal efficiency for acetochlor (93.1%) was achieved with the combination of photocatalyst P25 and reactor R1. However, the level of acetochlor removal by other photocatalysis experimental setups was considerably lower. The removal levels achieved for acetochlor after 180 min of photocatalytic reaction were 73.8%, 70.6%, and 77.4% when the process was carried out with P25/reactor R2, AV-01/reactor R1, and AV-01/reactor R2, respectively. In the case of photocatalyst AV-01, reactor R1 showed a slower degradation profile, which is consistent with the results obtained for alachlor. On the contrary, no significant differences were observed in the degradation profile in reactors R1 and R2 for the photocatalyst P25.

The highest metolachlor removal (98.2%) was achieved using photocatalyst P25 and reactor R2. However, an almost identical level of removal (97.9%) was obtained with photocatalyst AV-01 and reactor R1. The combination of photocatalyst P25 with reactor R1, and the combination of photocatalyst AV-01 with reactor R2 resulted in removal levels of 95.0% and 93.7%, respectively, in 180 min. In terms of degradation profile, opposite results were obtained compared to acetochlor. No significant differences in the degradation profile

were observed for photocatalyst P25 in reactors R1 and R2, whereas for photocatalyst P25, reactor R1 showed a slower degradation profile.

## 2.2. Toxicity Evaluation

### 2.2.1. Toxicity of Single Chloroacetanilide Herbicides

The toxicity of the chloroacetanilide herbicides alachlor, acetochlor, and metolachlor to the freshwater alga *Chlorella kessleri* was investigated via a growth inhibition test. After 72 h of exposure, the growth inhibition increased with the increasing concentration of herbicides in the exposure medium. The estimated dose–response curves depicting the course of the toxic effect of alachlor, acetochlor, and metolachlor on *Chlorella kessleri* are shown in Figure 2. The estimated dose–response curves for every single herbicide can be found in the Supplementary Material (see Figures S1–S3). The estimated values of 72 h EC<sub>50</sub> with 95% confidence intervals are summarized in Table 1. The results of toxicity testing in our study showed that *Chlorella kessleri* was the most vulnerable to the alachlor (14.07 µg/L), then to acetochlor (19.13 µg/L), and, in the presence of metolachlor, toxicity was an order of magnitude lower (115.10 µg/L). Our results showed that all herbicides were highly toxic to the freshwater alga *Chlorella kessleri*.

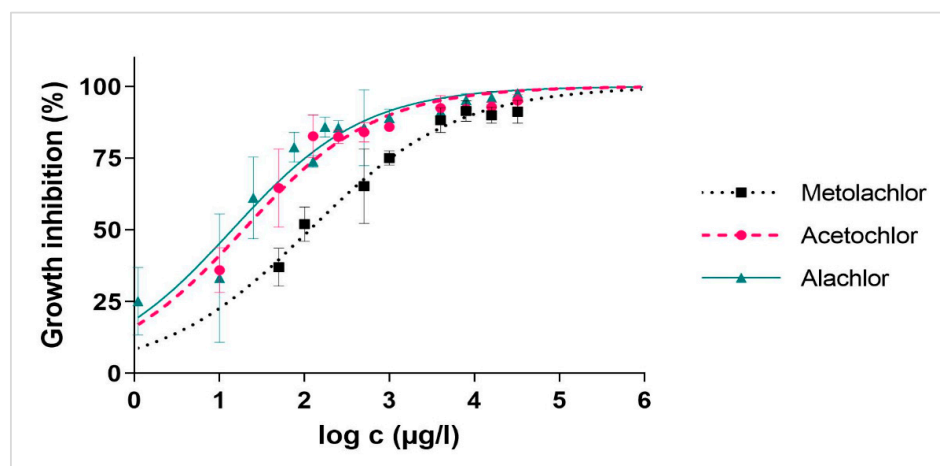


**Figure 2.** Estimation of dose–response curves describing the toxicity of tested chloroacetanilide herbicides to *Chlorella kessleri* after 72 h of exposure.

**Table 1.** Estimated 72 h EC<sub>50</sub> values (µg/L) of tested chloroacetanilide herbicides to *Chlorella kessleri* with 95% confidence intervals in brackets.

Chloroacetanilide Herbicide	Metolachlor	Acetochlor	Alachlor
72 h EC <sub>50</sub> (µg/L)	115.10 (86.19–148.50)	19.13 (13.25–25.71)	14.07 (9.59–19.66)

EC<sub>50</sub>—concentration inducing 50% effect growth inhibition.

### 2.2.2. Toxicity of Photocatalytic Degradation Products

The toxicity of mixtures of herbicides and their photocatalytic degradation products after 0 to 180 min of irradiation was investigated via a growth inhibition test. The dependences of the inhibition at different times of the photocatalysis in comparison with the average effectiveness of photocatalysis and concentration of herbicides in tests are shown in Figure 3. The graphs were created from average results obtained in individual photocatalysis modifications, which are reported in the Supplementary Material (see Figures S4–S6).

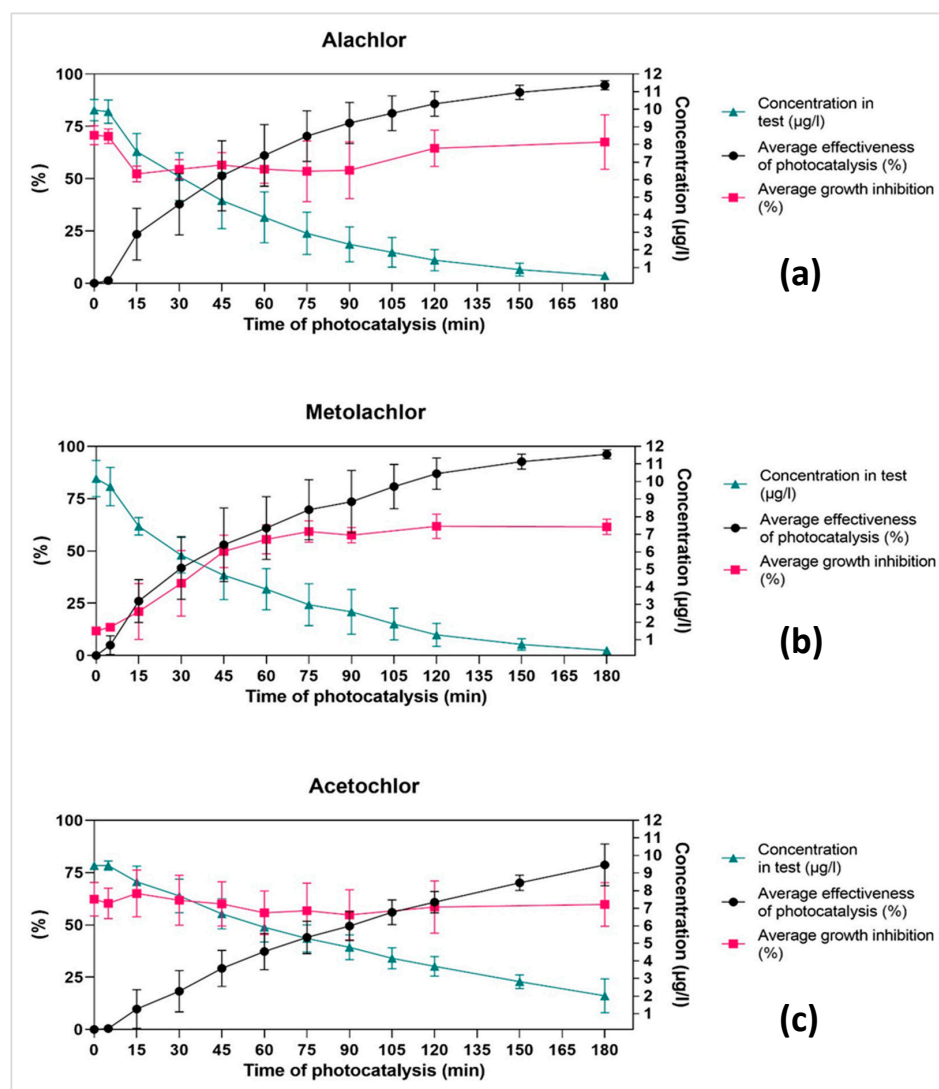


**Figure 3.** The average growth inhibition (%) of *Chlorella kessleri* exposed to a mixture of herbicides and their photocatalytic degradation products collected at a different time of photocatalysis (a point at the time of 5 min represents the time of contact of the photocatalyst with herbicides, but without irradiation) in comparison with the average effectiveness of photocatalysis and concentration of herbicides in tests (right axis): (a) alachlor, (b) metolachlor, (c) acetochlor.

The general expectation of this testing was that it would be possible to observe decreasing toxicity with decreasing herbicide concentration in the exposure medium. At the beginning of the photocatalysis, concentrations of herbicides (10 µg/L) were approximately at the EC<sub>50</sub> level of alachlor and acetochlor, and at EC<sub>25</sub> for metolachlor. However, after 72 h of exposure, the growth inhibition did not correlate with the concentration of any tested herbicide in the exposure medium (see Figure 3). Despite the fact that the concentrations of all herbicides during photocatalysis decreased, the toxicity of the resulting mixtures of herbicides and their photocatalytic degradation products increased (metolachlor) or remained the same (acetochlor), or slightly decreased, but then increased again (alachlor). It was found that the presence of the catalyst itself without irradiation has no significant effect on the concentration of herbicides or toxicity (a point at the time of 5 min). Interestingly, after 60 min of photocatalysis, the toxicity of all three herbicides was almost comparable, as can be seen in Figure 4. After 180 min of photocatalysis, the mixture of alachlor products still remained the most toxic. Observation suggests that the experimental design of photo-

catalysis likely led to products, other than monitored ethane sulfonic acids and oxanilic acids that influence growth of the alga more than primary herbicides.

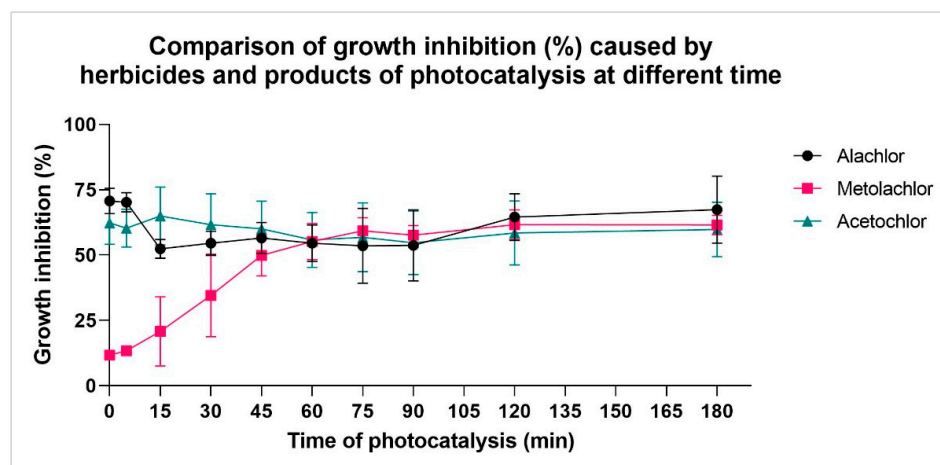


**Figure 4.** The average growth inhibition (%) of *Chlorella kessleri* exposed to a mixture of herbicides and their photocatalytic degradation products collected at a different time of photocatalysis.

### 3. Discussion

Heterogeneous photocatalysis using  $\text{TiO}_2/\text{UV}$  represents one of the most promising methods for combating environmental pollution with highly stable organic compounds [13,25]. Titanium dioxide is considered to be very close to an ideal semiconductor for photocatalysis, mainly due to its high photocatalytic stability, chemical inertness, low cost, and safety for humans and the environment [56,86]. Unlike some other semiconductors, such as ZnO, CdS, and GaP, which can dissolve and produce toxic by-products during the photocatalysis process,  $\text{TiO}_2$  itself remains unchanged during photocatalysis [23,87]. As a result, the photocatalyst can be regenerated for further use without a significant loss of catalytic activity [53]. Recyclability studies indicated effective reuse of  $\text{TiO}_2$ -based photocatalysts in multiple photocatalysis cycles [88–93].

Heterogeneous photocatalysis did not require consumable chemicals, which resulted in considerable material consumption and a simple operation of the process. Moreover, because the contaminant is strongly attracted to the surface of the photocatalyst, the degradation process will continue even at very low concentrations of the contaminant. These advantages resulted in low-cost and environmentally-friendly technology with high treatment efficiency [87].

Chloroacetanilide herbicides can be degraded by direct photolysis, as previously performed [7]. However, as reported [28], the photocatalysis of alachlor using  $\text{TiO}_2$  significantly improved the decay rate compared to direct photolysis. This is probably mainly due to the presence of a parallel (or additional) pathway of photocatalysis that coexists with direct photolysis.

According to our results, photocatalytic degradation using  $\text{TiO}_2/\text{UV}$  appears to be an effective strategy for the degradation of chloroacetanilide herbicides in water. Although our method eliminated all selected herbicides, the effectivity of photocatalytic degradations varied. From this point of view, the best results were achieved for metolachlor and alachlor. The use of P25 (90 mg/l) and UV-A for the photocatalytic degradation of an aqueous solution of metolachlor (5 mg/l) in a batch reactor has previously been reported. The removal efficiency after 60 minutes of irradiation was 88% [36]. The maximum removal efficiency of 98.44% was reported for alachlor using  $\text{TiO}_2$  nanoparticles as a photocatalyst under UV-C [13]. Even 100% removal of metolachlor was reported using a photocatalytically assisted ozone process with commercial P25 and synthesized  $\text{TiO}_2$  as photocatalysts [11].

On the contrary, acetochlor degradation was generally less successful, and the percentage efficiency of acetochlor removal at the end of the experiment (180 min) was, on

average, 20% lower compared to alachlor and metolachlor. This result can be derived from the different degradation rates during photocatalysis. The degradation rate of alachlor and metolachlor was higher in the first 90 min of the irradiation time, whereas in the second 90 min, the degradation rate gradually decreased. In contrast, the rate of acetochlor degradation was similar throughout the irrigation period. The dependence between removal efficiency and irradiation time was almost linear. This phenomenon was independent of the experimental setup used. In view of this fact, prolonging the irradiation time could result in an increase in acetochlor removal efficiency.

Ethane sulfonic acid and oxanilic acid are the most reported metabolites resulting from the degradation or mineralization of chloroacetanilide herbicides [94,95]. Ethane sulfonic acid is also the most abundant transformation product of chloroacetanilide herbicides found in soil [96]. Although the concentrations of these compounds in irradiated samples were monitored by the HPLC-MS-MS method, which allowed the monitoring of concentration levels of nanograms per liter, none of the compounds were detected, as their concentrations were below the limit of detection. These results indicate that ethane sulfonic acid and oxanilic acid were not the main degradation products of chloroacetanilide herbicides in this study.

In the present study, two commercially available  $\text{TiO}_2$  were used as photocatalysts. P25 is a well-characterized material with high photocatalytic activity, consisting of the anatase and rutile phase (80:20 or 70:30), representing the standard material in the field of photocatalytic reactions [30,97,98]. It was found that P25 exhibits higher photocatalytic activity than the other commercially available  $\text{TiO}_2$  photocatalysts. This is attributed to the mixed structure of P25  $\text{TiO}_2$  [53]. The rutile phase was found to not exist as an overlayer on the surface of the anatase particle, but it exists separately from the anatase particles [30]. The application of P25 as a photocatalyst for the photocatalytic degradation of alachlor [28,30] and metolachlor [36,39] has previously been reported. On the other hand, AV-01 is anatase titanium dioxide, used especially in paints, but also applicable for the pigmentation of rubber mixtures or direct injection into paper pulp. The present study reported the application of commercial  $\text{TiO}_2$  AV-01 as a photocatalyst for the first time. This material was selected considering the fact that the anatase phase of  $\text{TiO}_2$  is accepted as the most photoactive [13]. For this reason, we assumed that AV-01 could be used as a photocatalyst. This hypothesis was confirmed, since the degradation of chloroacetanilide herbicides carried out with AV-01 and P25 was comparable, and no significant differences were observed. Furthermore, similar to P25, AV-01 constitutes a relatively inexpensive, commercially available, and non-toxic material [98,99]. The non-toxicity of AV-01, as well as P25, was confirmed by the growth inhibition test with *Chlorella kessleri*. The addition of photocatalysts to the initial reaction solution did not increase the toxicity, because no significant variation in the percentage of growth inhibition was observed.

The effect of the reactor on degradation was also evaluated. It was assumed that a larger irradiated area in reactor R2 will ensure the improvement of degradation efficiencies due to the increase of the contact of the photocatalyst with photons. Although the degradation efficiency in reactor R2 was higher compared to reactor R1 in most of the experiments carried out, in some cases, the degradation profile was similar in both reactors. This could be caused by the inhomogeneity of the reaction solution during photocatalysis. Since reactor R2 had a rectangular cross-section compared to the square cross-section in reactor R1, the catalyst may not have been completely dispersed. As a result, the number of reaction sites could be limited.

Regarding the known toxicity of herbicides to non-target organisms, several studies on toxicity to aquatic organisms, including microalgae, can be found in the literature. The abundance, biomass, and growth rate are the most often studied toxicological parameters in tests with algae [100–103]. Few recent studies that try to address the mechanism of action can be found [3,6,12].

With regards to the  $\text{EC}_{50}$  values that can be found in the literature, values are in orders of micrograms of herbicides per liter, and range from units to hundreds depending on

the used alga and tested herbicide. It is known that algae and higher aquatic plants are more sensitive to the herbicides in comparison to other aquatic animals (such as daphnids, etc.), with  $EC_{50}$  values even three orders of magnitude lower [104]. For example, in a study with the green alga *Raphidocelis subcapitata*, 72 h  $EC_{50}$  46  $\mu\text{g/L}$  and 3  $\mu\text{g/L}$  for metolachlor and acetochlor were found, respectively [103], which are very similar values to ours. The authors also observed an order of magnitude difference in toxicity between metolachlor and acetochlor. Another study tested the toxicity of metolachlor to *Raphidocelis subcapitata* and after 48 h was estimated at 159  $\mu\text{g/L}$  as an  $EC_{50}$  and after 72 h, the value dropped to 98  $\mu\text{g/L}$  [105]. In another study with *Chlorella vulgaris*, the estimated 96 h  $EC_{50}$  values were 26  $\mu\text{g/L}$  and 84  $\mu\text{g/L}$  for alachlor and metolachlor, respectively [106]. Our experimentally detected values are, therefore, in accordance with those in the available literature.

Very little information exists about the toxicity of herbicide degradation products in the available literature. These products are rarely tested, even though these are commonly detected in the aquatic environment, and sometimes their concentrations are higher than the parent compounds [107]. In general, the toxicity of degradation products can be lower or similar to the parent compound, but in a third of available studies, there was an increase in the toxicity of degradation products [108]. As in our study, the increasing toxicity of degradation products can be found in a few studies [109–113]. For example, products of UV irradiation via modelled wastewater treatment of water containing alachlor, metolachlor, and acetochlor were tested on the freshwater microalga *Pseudokirchneriella subcapitata* [7]. In this study, the toxicity of the degradation products of all three herbicides was higher compared to the parent compounds. Similarly, another study also observed an increase in metolachlor toxicity to marine luminescence bacteria *Vibrio fischeri* using  $\text{TiO}_2$  as photocatalysts [36]. *Vibrio fischeri* was used in other available studies for the evaluation of the toxicity profile of herbicide clopyralid before and after its photocatalytic decomposition using  $\text{TiO}_2$  [114]. The authors observed increasing toxicity at the first stages of degradation, which they attribute to the progressive formation of intermediates more toxic than the parent molecule, or due to synergistic effects among the transformation products. However, the toxicity decreased eventually with increasing photocatalysis time.

## 4. Materials and Methods

### 4.1. Chemicals and Materials

Alachlor (99.2%), acetochlor (98.6%), metolachlor (97.9%), and their degradation products ethane sulfonic acid (ESA) and oxanilic acid (OA), were purchased from HPC Standards GmbH (Cunnersdorf, Germany). Commercial titanium dioxide, sample AEROXIDE<sup>®</sup>  $\text{TiO}_2$  P25 (specific surface area (BET) 35–65  $\text{m}^2/\text{g}$ ), was purchased from Evonik Industries AG (Hanau, Germany). Commercial titanium dioxide, sample PRETIOX<sup>®</sup>  $\text{TiO}_2$  AV-01 (specific surface area (BET) 11–15  $\text{m}^2/\text{g}$ ), was purchased from Precheza a.s. (Přerov, Czech Republic). For more information on the commercial titanium dioxides used, see the product information for AEROXIDE<sup>®</sup>  $\text{TiO}_2$  P25 and the product information for PRETIOX<sup>®</sup>  $\text{TiO}_2$  AV-01.

The chromatographic-grade solvents methanol and ammonium acetate were supplied by Sigma-Aldrich (St. Louis, MO, USA). Deionized water was produced by Milli-Q<sup>®</sup> Direct 8 Water Purification System (Merck KGaA, Darmstadt, Germany).

### 4.2. Photocatalytic Experiments

The photocatalytic degradation of alachlor, acetochlor, and metolachlor was performed in a batch lab-scale system which consisted of a stirred reaction vessel with a UV-A lamp with an irradiation intensity of 1284  $\text{W}/\text{cm}^2$  installed in the center above the reactor. The aqueous medium was represented by deionized water with a conductivity of less than 0.1  $\mu\text{S}/\text{cm}$ . In the experiments, two stainless steel reactors with varying dimensions were used. Reactor 1 (R1) had a volume of 2400 mL with dimensions of 176  $\times$  162 mm and a height of 150 mm, and the irradiated area was 285.12  $\text{cm}^2$ . Reactor 2 (R2) had a volume

of 4000 mL with dimensions of 265 × 162 mm and a height of 150 mm, and the irradiated area was 429.30 cm<sup>2</sup>.

Herbicide stock solutions (100 mg/L) were prepared in deionized water and stored in the dark at 4 °C. The reaction solution with a concentration of 10 mg/L was prepared from a stock solution of the appropriate chloroacetanilide herbicide by dilution in deionized water. The final volume of the herbicide solution treated was 1000 mL. The exact initial herbicide concentration was determined by HPLC-DAD. The reaction solution was magnetically stirred with a frequency of 500 rpm and heated to 25 °C using a Heidolph MR Hei-Tec magnetic stirrer (Heidolph Instruments GmbH & Co. KG, Schwabach, Germany).

At the beginning of the experiment, the initial herbicide solution was stirred vigorously for 5 min, and the initial sample was taken (marked 0—concentration of the herbicide at time 0 without the photocatalyst). Subsequently, the photocatalyst at a concentration of 1 g/L was added to the solution and dispersed for 5 min, and another sample (marked 0/TiO<sub>2</sub> concentration of the herbicide at time 0 with the photocatalyst) was taken. After this period, the UV-A lamp was switched on to initiate a photoreaction. For this study, two different commercial TiO<sub>2</sub> materials, P25 and AV-01, were tested. Each experiment was repeated three times.

During the experiment, 20 mL of the reaction solution was collected at regular time intervals of 15 min. The total duration of the experiment was 180 min. The collected samples were centrifuged at 11,000× g for 15 min to remove the photocatalyst using a centrifuge 5804 R (Eppendorf, Hamburg, Germany). The centrifuged samples were stored in the dark at 4 °C before further analysis. No sample processing was performed before HPLC analysis. For toxicity evaluation by the algae growth inhibition test, the samples were diluted a thousand times with sterile deionized water.

#### 4.3. Analytical Methods

Chloroacetanilide herbicide concentrations were monitored by HPLC-DAD, consisting of an Agilent 1260 Infinity II LC system equipped with a binary pump, an autosampler, and a WR diode array detector (Agilent Technologies, Santa Clara, CA, USA). Chromatograms were evaluated at 230 nm. Separation was carried out on a Kinetex C18 column (150 mm × 3 mm, particle size 2.6 μm) with a water/methanol gradient. The starting conditions for the mobile phase were set at 40% solvent A (water) and 60% solvent B (methanol). Within 10 min, solvent B was linearly increased to 100%, and kept constant for 5 min. Subsequently, the gradient was changed back to the initial conditions in 1 min. For the re-equilibration, these conditions were held for 4 min, resulting in a total run time of 20 min. The flow rate was set at 0.3 mL/min, the column temperature was maintained at 50 °C, and the injection volume was 50 μL.

The concentration of products, which resulted from photocatalytic degradation of chloroacetanilide herbicides, ethane sulfonic acid (ESA), and oxalic acid (OA), was monitored by HPLC-MS-MS. The HPLC system consisted of an Agilent 1260 Infinity II LC system equipped with a binary pump and an autosampler (Agilent Technologies, Santa Clara, CA, USA). The chromatographic column, temperature, and flow rate were the same as those for the HPLC-DAD analysis. The injection volume was 100 μL, and a water/methanol gradient was applied. The starting conditions for the mobile phase were set at 63% solvent A (water with 10 mM ammonium acetate) and 37% solvent B (methanol). Within 10 min, solvent B was linearly increased to 100%, and kept constant for 5 min. Subsequently, the gradient was changed back to the initial conditions in 1 min. For the re-equilibration, these conditions were held for 4 min, resulting in a total run time of 20 min. Detection was performed using the QTrap 4500 tandem mass spectrometric detector (Sciex, Framingham, MA, USA) equipped with electrospray ionization (ESI) and operated in positive mode. The optimized parameters related to the QqQ/MS experiments are shown in Table 2.

**Table 2.** Optimization of MS-MS conditions for the analysis of the photocatalysis degradation products.

Compound	MRM Transition	Declustering Potential DP (V)	Collision Energy CE (V)	Collision Cell Exit Potential CXP (V)
Alachlor OA	264/160	−20	−18	−5
Alachlor ESA	314/121	−35	−30	−7
Acetochlor OA	264/146	−30	−18	−5
Acetochlor ESA	314/80	−50	−68	−9
Metolachlor OA	278/206	−5	−16	−9
Metolachlor ESA	328/121	−55	−32	−7

ESA—ethane sulfonic acid; OA—oxanilic acid; MRM—multiple reaction monitoring.

#### 4.4. Algal Bioassay for Toxicity Determination

The freshwater chlorococcal alga *Chlorella kessleri* Fott *et* Novak (strain LARG/1) obtained from the Culture Collection of Autotrophic Organisms at the Institute of Botany in Třeboň (Czech Republic) was used as a test organism in this study. The growth inhibition test was performed according to the recommendations described in OECD 201 [115], but modified with respect to the use of the *Chlorella kessleri* strain. All operations were carried out under aseptic conditions to maintain the axenic culture. The OECD medium [115] and Bold's basal medium (BBM) [116] were used as growth media.

The stock culture was kept in 300 mL Erlenmeyer borosilicate flasks with a cotton top, containing 250 mL of OECD medium at  $26 \pm 2$  °C under a light (12 h) and dark (12 h) cycle with cool white light (luminescent tubes with a color temperature of 4300 K), with an intensity of 6000 lux on the surface of the flasks. Ten milliliters of stock culture was transferred weekly to 250 mL of fresh OECD medium to maintain the culture in the exponential growth phase.

##### 4.4.1. Microplate Bioassay

A miniaturized growth inhibition test in microplates was used to determine the toxicity of single chloroacetanilide herbicides. A preculture with an initial concentration of  $2 \times 10^5$  cells/mL was prepared from the stock culture 72 h before the start of the test. The precultures were incubated in 100 mL Erlenmeyer borosilicate flasks with a cotton top containing 50 mL of BMB medium under the same conditions as the test cultures. Incubation was carried out at  $22 \pm 2$  °C with agitation on an orbital shaker with a frequency of 150 rpm, in a thermostat with continuous cool white light (luminescent tubes with a color temperature of 4300 K) with an intensity of 8000 to 10,000 lux.

At the beginning of the toxicity test, the algal preculture in an exponential growth phase was diluted with a fresh BBM medium to achieve an initial cell density of  $2 \times 10^5$  cells/mL. Toxicity tests were performed in 96-well polystyrene sterile microplates with a flat bottom. Per well, a volume of 225  $\mu$ L of algal suspension and 25  $\mu$ L of herbicide stock solution was used. As a control, the algal suspension was only incubated in BBM medium. The final test volume was 250  $\mu$ L per well. The tests were run for 72 h under the conditions described above for precultures. During incubation, microplates were covered with clear polystyrene lids to prevent air contamination and evaporation of the growth medium.

After 72 h of exposure, cell density was determined by the measurement of optical density at 684 nm ( $OD_{684}$ ) using a microplate spectrophotometer, Epoch (BioTek Instruments, Winooski, VT, USA).

The geometric series of nine equally-spaced concentrations of each herbicide was tested first. The concentration range of 0.125–32 mg/L with factor 2 was tested for all chloroacetanilide herbicides. Each concentration was tested in five replicates, and similarly, a growth control was tested in five replicates. For each herbicide, three independent series of assays were performed. Lower concentrations were subsequently tested for

EC<sub>50</sub> determination (0.125–0.001 mg/L). The results from three-times repeated tests were averaged and used for EC<sub>50</sub> calculations and the creation of dose–response curves.

#### 4.4.2. Flask Bioassay

A flask growth inhibition test was used to evaluate the toxicity of herbicide mixtures and their photocatalytic degradation products collected at different time intervals during photocatalysis. Due to the concentration of herbicides in the initial reaction solution (10 mg/L), the samples were diluted (1000 times) with sterile deionized water to obtain concentrations approximately corresponding to the estimated values of EC<sub>50</sub> of chloroacetanilide herbicides.

A preculture with an initial concentration of  $5 \times 10^4$  cells/mL was prepared from the stock culture 72 h before the start of the test. The precultures were incubated in 300 mL Erlenmeyer borosilicate flasks with a cotton top containing 250 mL of OECD medium under the same conditions as the test cultures. Incubation was carried out at  $28 \pm 2$  °C with agitation on an orbital shaker with a frequency of 120 rpm in a temperature-controlled culture box under a light (18 h) and dark (16 h) cycle with cool white light (luminescent tubes with a color temperature of 4300 K) with an intensity of 8000 to 10,000 lux.

At the beginning of the toxicity test, the algal preculture in an exponential growth phase was diluted with a fresh OECD medium to achieve an initial cell density of  $5 \times 10^4$  cells/mL. The toxicity tests were performed in 30 mL volumes in 50 mL sterile Erlenmeyer borosilicate flasks. As a control, the algal suspension was incubated in an OECD medium. The tests were run for 72 h under the conditions described above for precultures. The flask neck was covered with cellulose wadding to prevent air contamination and evaporation of the growth medium.

After 72 h of exposure, cell density was determined by the measurement of optical density at 684 nm (OD<sub>684</sub>) using a DR6000 spectrophotometer (Hach Lange, Düsseldorf, Germany). The three replicates of each sample were tested. Growth controls were tested in five replicates.

#### 4.4.3. Data Analysis

Growth rates and percentage inhibition were calculated according to OECD 201 [115]. The percentage inhibition of the growth rate was plotted against the time of treatment to evaluate the changes in acute toxicity of the irradiated solution during photocatalysis.

The dose–response curves and EC<sub>50</sub> calculations (growth inhibition concentration) were made using a non-linear curve fitting procedure in the GraphPad 9 statistical software (Version for Windows, GraphPad Software, San Diego, CA, USA). The best-fitting model for experimental data was log vs. normalized response with variable slope, and the equations had the form:  $Y = 100 / (1 + 10^{((\text{LogEC}_{50} - X) \cdot \text{HillSlope}))}$ , in which Y is the inhibition (% of control value), HillSlope is the slope, and X is log concentration (mg/L).

## 5. Conclusions

The present study focuses on the photocatalytic degradation of the chloroacetanilide herbicides alachlor, acetochlor, and metolachlor with TiO<sub>2</sub>/UV-A. The results demonstrate that titania-mediated photocatalytic is an efficient process for the removal of chloroacetanilide herbicides from an aqueous solution. Two commercial TiO<sub>2</sub> materials were used as photocatalysts: P25, as the standard for photocatalytic applications; and AV-01, which is reported as a photocatalyst for the first time. However, it was confirmed that the anatase titanium dioxide AV-01 has photocatalytic activity and can be successfully applied as a photocatalyst.

Although the maximum removal efficiency for alachlor, acetochlor, and metolachlor was 97.5%, 93.1%, and 98.2%, respectively, it was not enough for toxicity abatement. First, our results showed that all investigated herbicides are highly toxic to the freshwater alga *Chlorella kessleri*. Furthermore, the toxicity of the resulting mixtures of herbicides and their

photocatalysis degradation products increased or remained the same as that of the initial herbicide solutions.

This phenomenon can be ascribed to the formation of degradation products of the same or even more toxic nature in comparison to the parent compounds. The fact that none of the major metabolites resulting from the degradation of chloroacetanilide herbicides was detected indicates the complexity of the photocatalytic process, and the existence of various degradation routes resulting in a complex mixture of degradation products. For this reason, toxicity monitoring can contribute to the evaluation of efficiency and subsequent optimization of the photocatalysis process.

**Supplementary Materials:** The following supporting information can be downloaded at: <https://www.mdpi.com/article/10.3390/catal12060597/s1>, Figure S1: Estimation of dose–response curves describing the acute toxicity of metolachlor to *Chlorella kessleri* after 72 h of exposure, Figure S2: Estimation of dose–response curves describing the acute toxicity of acetochlor to *Chlorella kessleri* after 72 h of exposure, Figure S3: Estimation of dose–response curves describing the acute toxicity of alachlor to *Chlorella kessleri* after 72 h of exposure, Figure S4: The dependence of the *Chlorella kessleri* growth inhibition (%) at different times of the metolachlor photocatalysis on the used catalyst and reactor vessel, Figure S5: The dependence of the *Chlorella kessleri* growth inhibition (%) at different times of the acetochlor photocatalysis on the used catalyst and reactor vessel, Figure S6: The dependence of the *Chlorella kessleri* growth inhibition (%) at different times of the alachlor photocatalysis on the used catalyst and reactor vessel.

**Author Contributions:** Conceptualization, P.P. and J.P.; Funding acquisition, J.P.; Investigation, N.R., K.H., M.K., P.P., D.J. and J.P.; Methodology, N.R., K.H., M.K., P.P. and J.P.; Project administration, J.P.; Supervision, J.P.; Visualization, N.R., K.H., M.K. and J.P.; Writing—original draft, N.R., K.H., M.K. and J.P.; Writing—review and editing, N.R., K.H., M.K. and J.P. All authors have read and agreed to the published version of the manuscript.

**Funding:** This research was funded by the Technology Agency of the Czech Republic, a program for the funding of applied research ZETA, project name: Combined procedure of elimination of chloroacetanilide pesticides from contaminated water and soil, grant number: TJ04000226.

**Data Availability Statement:** The data presented in this study are available on request from the corresponding author.

**Conflicts of Interest:** The authors declare no conflict of interest.

## References

1. Mohanty, S.S.; Jena, H.M. A systemic assessment of the environmental impacts and remediation strategies for chloroacetanilide herbicides. *J. Water Process. Eng.* **2019**, *31*, 100860. [[CrossRef](#)]
2. Huang, T.; Huang, Y.; Huang, Y.; Yang, Y.; Zhao, Y.; Martyniuk, C.J. Toxicity assessment of the herbicide acetochlor in the human liver carcinoma (HepG2) cell line. *Chemosphere* **2020**, *243*, 125345. [[CrossRef](#)] [[PubMed](#)]
3. Machado, M.D.; Soares, E.V. Exposure of the alga *Pseudokirchneriella subcapitata* to environmentally relevant concentrations of the herbicide metolachlor: Impact on the redox homeostasis. *Ecotoxicol. Environ. Saf.* **2021**, *207*, 111264. [[CrossRef](#)] [[PubMed](#)]
4. Thiam, A.; Salazar, R. Fenton-based electrochemical degradation of metolachlor in aqueous solution by means of BDD and Pt electrodes: Influencing factors and reaction pathways. *Environ. Sci. Pollut. Res.* **2019**, *26*, 2580–2591. [[CrossRef](#)] [[PubMed](#)]
5. Sigurnjak, M.; Ukić, Š.; Cvetnić, M.; Markić, M.; Novak Stankov, M.; Rasulev, B.; Kušić, H.; Lončarić Božić, A.; Rogošić, M.; Bolanča, T. Combined toxicities of binary mixtures of alachlor, chlorfenvinphos, diuron and isoproturon. *Chemosphere* **2020**, *240*, 124973. [[CrossRef](#)]
6. Machado, M.D.; Soares, E.V. Reproductive cycle progression arrest and modification of cell morphology (shape and biovolume) in the alga *Pseudokirchneriella subcapitata* exposed to metolachlor. *Aquat. Toxicol.* **2020**, *222*, 105449. [[CrossRef](#)]
7. Souissi, Y.; Bouchonnet, S.; Bourcier, S.; Kusk, K.O.; Sablier, M.; Andersen, H.R. Identification and ecotoxicity of degradation products of chloroacetamide herbicides from UV-treatment of water. *Sci. Total Environ.* **2013**, *458–460*, 527–534. [[CrossRef](#)]
8. Chen, Z.; Chen, Y.; Vymazal, J.; Kule, L.; Koželuh, M. Dynamics of chloroacetanilide herbicides in various types of mesocosm wetlands. *Sci. Total Environ.* **2017**, *577*, 386–394. [[CrossRef](#)]
9. Debenest, T.; Silvestre, J.; Coste, M.; Pinelli, E. Effects of pesticides on freshwater diatoms. *Rev. Environ. Contam. Toxicol.* **2010**, *203*, 87–103. [[CrossRef](#)]
10. Abigail, M.E.A.; Samuel, S.M.; Ramalingam, C. Addressing the environmental impacts of butachlor and the available remediation strategies: A systematic review. *Int. J. Environ. Sci. Technol.* **2015**, *12*, 4025–4036. [[CrossRef](#)]

11. Orge, C.A.; Pereira, M.F.R.; Faria, J.L. Photocatalytic-assisted ozone degradation of metolachlor aqueous solution. *Chem. Eng. J.* **2017**, *318*, 247–253. [[CrossRef](#)]
12. Kim, H.; Wang, H.; Ki, J.S. Chloroacetanilides inhibit photosynthesis and disrupt the thylakoid membranes of the dinoflagellate *Prorocentrum minimum* as revealed with metazachlor treatment. *Ecotoxicol. Environ. Saf.* **2021**, *211*, 111928. [[CrossRef](#)] [[PubMed](#)]
13. Jamshidi, F.; Dehghani, M.; Yousefinejad, S.; Azhdarpoor, A. Photocatalytic degradation of alachlor by TiO<sub>2</sub> nanoparticles from aqueous solutions under UV radiation. *J. Exp. Nanosci.* **2019**, *14*, 116–128. [[CrossRef](#)]
14. Liu, J.; Zhang, X.; Xu, J.; Qiu, J.; Zhu, J.; Cao, H.; He, J. Anaerobic biodegradation of acetochlor by acclimated sludge and its anaerobic catabolic pathway. *Sci. Total Environ.* **2020**, *748*, 141122. [[CrossRef](#)]
15. Machado, M.D.; Soares, E.V. Sensitivity of freshwater and marine green algae to three compounds of emerging concern. *J. Appl. Phycol.* **2019**, *31*, 399–408. [[CrossRef](#)]
16. Gar Alalm, M.; Tawfik, A.; Ookawara, S. Comparison of solar TiO<sub>2</sub> photocatalysis and solar photo-Fenton for treatment of pesticides industry wastewater: Operational conditions, kinetics, and costs. *J. Water Process. Eng.* **2015**, *8*, 55–63. [[CrossRef](#)]
17. Gar Alalm, M.G.; Tawfik, A.; Ookawara, S. Combined solar advanced oxidation and PAC adsorption for removal of pesticides from industrial wastewater. *J. Mater. Environ. Sci.* **2015**, *6*, 800–809.
18. Lou, Y.Y.; Geneste, F.; Soutrel, I.; Amrane, A.; Fourcade, F. Alachlor dechlorination prior to an electro-Fenton process: Influence on the biodegradability of the treated solution. *Sep. Purif. Technol.* **2020**, *232*, 115936. [[CrossRef](#)]
19. Wang, J.; Zhuang, R. Degradation of antibiotics by advanced oxidation processes: An overview. *Sci. Total Environ.* **2020**, *701*, 135023. [[CrossRef](#)]
20. Aziz, K.H.H.; Omer, K.M.; Mahyar, A.; Miessner, H.; Mueller, S.; Moeller, D. Application of photocatalytic falling film reactor to elucidate the degradation pathways of pharmaceutical diclofenac and ibuprofen in aqueous solutions. *Coatings* **2019**, *9*, 465. [[CrossRef](#)]
21. Cuerda-Correa, E.M.; Alexandre-Franco, M.F.; Fernández-González, C. Advanced oxidation processes for the removal of antibiotics from water. An overview. *Water* **2020**, *12*, 102. [[CrossRef](#)]
22. Stan, C.D.; Cretescu, I.; Pastravanu, C.; Poullos, I.; Drăgan, M. Treatment of pesticides in wastewater by heterogeneous and homogeneous photocatalysis. *Int. J. Photoenergy* **2012**, *2012*, 194823. [[CrossRef](#)]
23. Cheng, M.; Zeng, G.; Huang, D.; Lai, C.; Xu, P.; Zhang, C.; Liu, Y. Hydroxyl radicals based advanced oxidation processes (AOPs) for remediation of soils contaminated with organic compounds: A review. *Chem. Eng. J.* **2016**, *284*, 582–598. [[CrossRef](#)]
24. Lee, C.M.; Palaniandy, P.; Dahlan, I. Pharmaceutical residues in aquatic environment and water remediation by TiO<sub>2</sub> heterogeneous photocatalysis: A review. *Environ. Earth Sci.* **2017**, *76*, 611. [[CrossRef](#)]
25. Isari, A.A.; Payan, A.; Fattahi, M.; Jorfi, S.; Kakavandi, B. Photocatalytic degradation of rhodamine B and real textile wastewater using Fe-doped TiO<sub>2</sub> anchored on reduced graphene oxide (Fe-TiO<sub>2</sub>/rGO): Characterization and feasibility, mechanism and pathway studies. *Appl. Surf. Sci.* **2018**, *462*, 549–564. [[CrossRef](#)]
26. Hu, N.; Xu, Y.; Sun, C.; Zhu, L.; Sun, S.; Zhao, Y.; Hu, C. Removal of atrazine in catalytic degradation solutions by microalgae *Chlorella* sp. and evaluation of toxicity of degradation products via algal growth and photosynthetic activity. *Ecotoxicol. Environ. Saf.* **2021**, *207*, 111546. [[CrossRef](#)]
27. Mbiri, A.; Wittstock, G.; Taffa, D.H.; Gatebe, E.; Baya, J.; Wark, M. Photocatalytic degradation of the herbicide chloridazon on mesoporous titania/zirconia nanopowders. *Environ. Sci. Pollut. Res.* **2018**, *25*, 34873–34883. [[CrossRef](#)]
28. Wong, C.C.; Chu, W. The direct photolysis and photocatalytic degradation of alachlor at different TiO<sub>2</sub> and UV sources. *Chemosphere* **2003**, *50*, 981–987. [[CrossRef](#)]
29. de Luna, M.D.G.; Rivera, K.K.P.; Suwannaruang, T.; Wantala, K. Alachlor photocatalytic degradation over uncalcined Fe–TiO<sub>2</sub> loaded on granular activated carbon under UV and visible light irradiation. *Desalination Water Treat.* **2016**, *57*, 6712–6722. [[CrossRef](#)]
30. Malini, T.P.; Ramesh, A.; Selvi, J.A.; Arthanareeswari, M.; Kamaraj, P. Kinetic modeling of photocatalytic degradation of alachlor using TiO<sub>2</sub> (Degussa P25) in aqueous solution. *Orient. J. Chem.* **2016**, *32*, 3165–3173. [[CrossRef](#)]
31. Rivera, K.K.P.; de Luna, M.D.G.; Suwannaruang, T.; Wantala, K. Photocatalytic degradation of reactive red 3 and alachlor over uncalcined Fe–TiO<sub>2</sub> synthesized via hydrothermal method. *Desalin. Water Treat.* **2016**, *57*, 22017–22028. [[CrossRef](#)]
32. Suwannaruang, T.; Wantala, K. Single-step uncalcined N-TiO<sub>2</sub> synthesis, characterizations and its applications on alachlor photocatalytic degradations. *Appl. Surf. Sci.* **2016**, *380*, 257–267. [[CrossRef](#)]
33. Zheng, D.; Xin, Y.; Ma, D.; Wang, X.; Wu, J.; Gao, M. Preparation of graphene/TiO<sub>2</sub> nanotube array photoelectrodes and their photocatalytic activity for the degradation of alachlor. *Catal. Sci. Technol.* **2016**, *6*, 1892–1902. [[CrossRef](#)]
34. Molla, M.; Furukawa, M.; Tateishi, I.; Katsumata, H.; Kaneco, S. Optimization of Alachlor Photocatalytic Degradation with Nano-TiO<sub>2</sub> in Water under Solar Illumination: Reaction Pathway and Mineralization. *Clean Technol.* **2018**, *1*, 141–153. [[CrossRef](#)]
35. Pérez, M.H.; Vega, L.P.; Zúñiga-Benítez, H.; Peñuela, G.A. Comparative Degradation of Alachlor Using Photocatalysis and Photo-Fenton. *Water Air Soil Pollut.* **2018**, *229*, 346. [[CrossRef](#)]
36. Sakkas, V.A.; Arabatzis, I.M.; Konstantinou, I.K.; Dimou, A.D.; Albanis, T.A.; Falaras, P. Metolachlor photocatalytic degradation using TiO<sub>2</sub> photocatalysts. *Appl. Catal. B* **2004**, *49*, 195–205. [[CrossRef](#)]
37. Peng, Y.-Z.; Ma, W.-H.; Jia, M.-K.; Zhao, X.-R.; Johnson, D.M.; Huang, Y.-P. Comparing the degradation of acetochlor to RhB using BiOBr under visible light: A significantly different rate-catalyst dose relationship. *Appl. Catal. B* **2016**, *181*, 517–523. [[CrossRef](#)]

38. Mermana, J.; Sutthivaiyakit, P.; Blaise, C.; Gagné, F.; Charnsethikul, S.; Kidkhunthod, P.; Sutthivaiyakit, S. Photocatalysis of S-metolachlor in aqueous suspension of magnetic cerium-doped mTiO<sub>2</sub> core-shell under simulated solar light. *Environ. Sci. Pollut. Res.* **2017**, *24*, 4077–4092. [[CrossRef](#)]
39. Rancaño, L.; Rivero, M.J.; Mueses, M.Á.; Ortiz, I. Comprehensive kinetics of the photocatalytic degradation of emerging pollutants in a LED-assisted photoreactor: S-metolachlor as case study. *Catalysts* **2021**, *11*, 48. [[CrossRef](#)]
40. Li, H.Y.; Qu, J.H.; Zhao, X.; Liu, H.J. Removal of alachlor from water by catalyzed ozonation in the presence of Fe<sup>2+</sup>, Mn<sup>2+</sup>, and humic substances. *J. Environ. Sci. Health-B Pestic. Food Contam. Agric. Wastes* **2004**, *39*, 791–803. [[CrossRef](#)]
41. Qiang, Z.; Liu, C.; Dong, B.; Zhang, Y. Degradation mechanism of alachlor during direct ozonation and O<sub>3</sub>/H<sub>2</sub>O<sub>2</sub> advanced oxidation process. *Chemosphere* **2010**, *78*, 517–526. [[CrossRef](#)] [[PubMed](#)]
42. Li, H.; Huang, Y.; Cui, S. Removal of alachlor from water by catalyzed ozonation on Cu/Al<sub>2</sub>O<sub>3</sub> honeycomb. *Chem. Cent. J.* **2013**, *7*, 143. [[CrossRef](#)] [[PubMed](#)]
43. Katsumata, H.; Kaneco, S.; Suzuki, T.; Ohta, K.; Yobiko, Y. Photo-Fenton degradation of alachlor in the presence of citrate solution. *J. Photochem. Photobiol. A Chem.* **2006**, *180*, 38–45. [[CrossRef](#)]
44. Pipi, A.R.F.; De Andrade, A.R.; Brillas, E.; Sirés, I. Total removal of alachlor from water by electrochemical processes. *Sep. Purif. Technol.* **2014**, *132*, 674–683. [[CrossRef](#)]
45. Wardenier, N.; Liu, Z.; Nikiforov, A.; Van Hulle, S.W.H.; Leys, C. Micropollutant elimination by O<sub>3</sub>, UV and plasma-based AOPs: An evaluation of treatment and energy costs. *Chemosphere* **2019**, *234*, 715–724. [[CrossRef](#)]
46. Wardenier, N.; Gorbanev, Y.; Van Moer, I.; Nikiforov, A.; Van Hulle, S.W.H.; Surmont, P.; Lynen, F.; Leys, C.; Bogaerts, A.; Vanraes, P. Removal of alachlor in water by non-thermal plasma: Reactive species and pathways in batch and continuous process. *Water Res.* **2019**, *161*, 549–559. [[CrossRef](#)]
47. Acero, J.L.; Benitez, F.J.; Real, F.J.; Maya, C. Oxidation of Acetamide Herbicides in Natural Waters by Ozone and by the Combination of Ozone/Hydrogen Peroxide: Kinetic Study and Process Modeling. *Ind. Eng. Chem. Res.* **2003**, *42*, 5762–5769. [[CrossRef](#)]
48. Restivo, J.; Órfão, J.J.M.; Armenise, S.; Garcia-Bordejé, E.; Pereira, M.F.R. Catalytic ozonation of metolachlor under continuous operation using nanocarbon materials grown on a ceramic monolith. *J. Hazard. Mater.* **2012**, *239–240*, 249–256. [[CrossRef](#)]
49. Wang, J.; Lou, Y.; Zhuang, X.; Song, S.; Liu, W.; Xu, C. Magnetic Pr<sub>6</sub>O<sub>11</sub>/SiO<sub>2</sub>@Fe<sub>3</sub>O<sub>4</sub> particles as the heterogeneous catalyst for the catalytic ozonation of acetochlor: Performance and aquatic toxicity. *Sep. Purif. Technol.* **2018**, *197*, 63–69. [[CrossRef](#)]
50. Huston, P.L.; Pignatello, J.J. Degradation of selected pesticide active ingredients and commercial formulations in water by the photo-assisted Fenton reaction. *Water Res.* **1999**, *33*, 1238–1246. [[CrossRef](#)]
51. Benzaquén, T.B.; Benzzo, M.T.; Isla, M.A.; Alfano, O.M. Impact of some herbicides on the biomass activity in biological treatment plants and biodegradability enhancement by a photo-Fenton process. *Water Sci. Technol.* **2013**, *67*, 210–216. [[CrossRef](#)] [[PubMed](#)]
52. Guelfi, D.R.V.; Gozzi, F.; Machulek, A.; Sirés, I.; Brillas, E.; de Oliveira, S.C. Degradation of herbicide S-metolachlor by electrochemical AOPs using a boron-doped diamond anode. *Catal. Today* **2018**, *313*, 182–188. [[CrossRef](#)]
53. Mahmoud, W.M.M.; Rastogi, T.; Kümmerer, K. Application of titanium dioxide nanoparticles as a photocatalyst for the removal of micropollutants such as pharmaceuticals from water. *Curr. Opin. Green Sustain. Chem.* **2017**, *6*, 1–10. [[CrossRef](#)]
54. Reghunath, S.; Pinheiro, D.; KR, S.D. A review of hierarchical nanostructures of TiO<sub>2</sub>: Advances and applications. *Appl. Surf. Sci.* **2021**, *3*, 100063. [[CrossRef](#)]
55. Serga, V.; Burve, R.; Krumina, A.; Romanova, M.; Kotomin, E.A.; Popov, A.I. Extraction-pyrolytic method for TiO<sub>2</sub> polymorphs production. *Crystals* **2021**, *11*, 431. [[CrossRef](#)]
56. Gupta, S.M.; Tripathi, M. A review of TiO<sub>2</sub> nanoparticles. *Sci. Bull.* **2011**, *56*, 1639–1657. [[CrossRef](#)]
57. Kang, X.; Liu, S.; Dai, Z.; He, Y.; Song, X.; Tan, Z. Titanium dioxide: From engineering to applications. *Catalysts* **2019**, *9*, 191. [[CrossRef](#)]
58. Li, R.; Li, T.; Zhou, Q. Impact of titanium dioxide (TiO<sub>2</sub>) modification on its application to pollution treatment—A review. *Catalysts* **2020**, *10*, 804. [[CrossRef](#)]
59. Nguyen, V.H.; Smith, S.M.; Wantala, K.; Kajitvichyanukul, P. Photocatalytic remediation of persistent organic pollutants (POPs): A review. *Arab. J. Chem.* **2020**, *13*, 8309–8337. [[CrossRef](#)]
60. Lopes, J.Q.; Cardeal, R.A.; Araújo, R.D.S.; Assunção, J.C.D.C.; Salgado, B.C.B. Application of titanium dioxide as photocatalyst in diuron degradation: Operational variables evaluation and mechanistic study. *Eng. Sanit. Ambient.* **2021**, *26*, 61–68. [[CrossRef](#)]
61. Andersen, J.; Pelaez, M.; Guay, L.; Zhang, Z.; O’Shea, K.; Dionysiou, D.D. NF-TiO<sub>2</sub> photocatalysis of amitrole and atrazine with addition of oxidants under simulated solar light: Emerging synergies, degradation intermediates, and reusable attributes. *J. Hazard. Mater.* **2013**, *260*, 569–575. [[CrossRef](#)] [[PubMed](#)]
62. Gholami, M.; Shirzad-Siboni, M.; Farzadkia, M.; Yang, J.K. Synthesis, characterization, and application of ZnO/TiO<sub>2</sub> nanocomposite for photocatalysis of a herbicide (Bentazon). *Desalin. Water Treat.* **2016**, *57*, 13632–13644. [[CrossRef](#)]
63. Le Cunff, J.; Tomašić, V.; Wittine, O. Photocatalytic degradation of the herbicide terbuthylazine: Preparation, characterization and photoactivity of the immobilized thin layer of TiO<sub>2</sub>/chitosan. *J. Photochem. Photobiol. A Chem.* **2015**, *309*, 22–29. [[CrossRef](#)]
64. Fiorenza, R.; Di Mauro, A.; Cantarella, M.; Gulino, A.; Spitaleri, L.; Privitera, V.; Impellizzeri, G. Molecularly imprinted N-doped TiO<sub>2</sub> photocatalysts for the selective degradation of o-phenylphenol fungicide from water. *Mater. Sci. Semicond. Process.* **2020**, *112*, 105019. [[CrossRef](#)]

65. Berberidou, C.; Kitsiou, V.; Lambropoulou, D.A.; Michailidou, D.; Kouras, A.; Poullos, I. Decomposition and detoxification of the insecticide thiacloprid by TiO<sub>2</sub>-mediated photocatalysis: Kinetics, intermediate products and transformation pathways. *J. Chem. Technol. Biotechnol.* **2019**, *94*, 2475–2486. [[CrossRef](#)]
66. Borges, M.E.; García, D.M.; Hernández, T.; Ruiz-Morales, J.C.; Esparza, P. Supported photocatalyst for removal of emerging contaminants from wastewater in a continuous packed-bed photoreactor configuration. *Catalysts* **2015**, *5*, 77–87. [[CrossRef](#)]
67. Hashim, N.; Thakur, S.; Patang, M.; Crapulli, F.; Ray, A.K. Solar degradation of diclofenac using Eosin-Y-activated TiO<sub>2</sub>: Cost estimation, process optimization and parameter interaction study. *Environ. Technol.* **2017**, *38*, 933–944. [[CrossRef](#)]
68. Jallouli, N.; Pastrana-Martínez, L.M.; Ribeiro, A.R.; Moreira, N.F.F.; Faria, J.L.; Hentati, O.; Silva, A.M.T.; Ksibi, M. Heterogeneous photocatalytic degradation of ibuprofen in ultrapure water, municipal and pharmaceutical industry wastewaters using a TiO<sub>2</sub>/UV-LED system. *Chem. Eng. J.* **2018**, *334*, 976–984. [[CrossRef](#)]
69. Zheng, X.; Xu, S.; Wang, Y.; Sun, X.; Gao, Y.; Gao, B. Enhanced degradation of ciprofloxacin by graphitized mesoporous carbon (GMC)-TiO<sub>2</sub> nanocomposite: Strong synergy of adsorption-photocatalysis and antibiotics degradation mechanism. *J. Colloid Interface Sci.* **2018**, *527*, 202–213. [[CrossRef](#)]
70. Biancullo, F.; Moreira, N.F.F.; Ribeiro, A.R.; Manaia, C.M.; Faria, J.L.; Nunes, O.C.; Castro-Silva, S.; Silva, A.M.T. Heterogeneous photocatalysis using UVA-LEDs for the removal of antibiotics and antibiotic resistant bacteria from urban wastewater treatment plant effluents. *Chem. Eng. J.* **2019**, *367*, 304–313. [[CrossRef](#)]
71. Cai, Q.; Hu, J. Decomposition of sulfamethoxazole and trimethoprim by continuous UVA/LED/TiO<sub>2</sub> photocatalysis: Decomposition pathways, residual antibacterial activity and toxicity. *J. Hazard. Mater.* **2017**, *323*, 527–536. [[CrossRef](#)] [[PubMed](#)]
72. Luo, Z.; Li, L.; Wei, C.; Li, H.; Chen, D. Role of active oxidative species on TiO<sub>2</sub> photocatalysis of tetracycline and optimization of photocatalytic degradation conditions. *J. Environ. Biol.* **2015**, *36*, 837–843. [[PubMed](#)]
73. Guo, C.; Wang, K.; Hou, S.; Wan, L.; Lv, J.; Zhang, Y.; Qu, X.; Chen, S.; Xu, J. H<sub>2</sub>O<sub>2</sub> and/or TiO<sub>2</sub> photocatalysis under UV irradiation for the removal of antibiotic resistant bacteria and their antibiotic resistance genes. *J. Hazard. Mater.* **2017**, *323*, 710–718. [[CrossRef](#)] [[PubMed](#)]
74. Asencios, Y.J.O.; Lourenço, V.S.; Carvalho, W.A. Removal of phenol in seawater by heterogeneous photocatalysis using activated carbon materials modified with TiO<sub>2</sub>. *Catal. Today* **2022**, *388–389*, 247–258. [[CrossRef](#)]
75. Lopes da Silva, F.; Laitinen, T.; Pirilä, M.; Keiski, R.L.; Ojala, S. Photocatalytic Degradation of Perfluorooctanoic Acid (PFOA) From Wastewaters by TiO<sub>2</sub>, In<sub>2</sub>O<sub>3</sub> and Ga<sub>2</sub>O<sub>3</sub> Catalysts. *Top. Catal.* **2017**, *60*, 1345–1358. [[CrossRef](#)]
76. Nguyen, C.H.; Tran, M.L.; Tran, T.T.V.; Juang, R.S. Enhanced removal of various dyes from aqueous solutions by UV and simulated solar photocatalysis over TiO<sub>2</sub>/ZnO/rGO composites. *Sep. Purif. Technol.* **2020**, *232*, 115962. [[CrossRef](#)]
77. Nyankson, E.; Efavi, J.K.; Agyei-Tuffour, B.; Manu, G. Synthesis of TiO<sub>2</sub>-Ag<sub>3</sub>PO<sub>4</sub> photocatalyst material with high adsorption capacity and photocatalytic activity: Application in the removal of dyes and pesticides. *RSC Adv.* **2021**, *11*, 17032–17045. [[CrossRef](#)]
78. Domínguez-Jaimes, L.P.; Cedillo-González, E.I.; Luévano-Hipólito, E.; Acuña-Bedoya, J.D.; Hernández-López, J.M. Degradation of primary nanoplastics by photocatalysis using different anodized TiO<sub>2</sub> structures. *J. Hazard. Mater.* **2021**, *413*, 125452. [[CrossRef](#)]
79. Babu, D.S.; Srivastava, V.; Nidheesh, P.V.; Kumar, M.S. Detoxification of water and wastewater by advanced oxidation processes. *Sci. Total Environ.* **2019**, *696*, 133961. [[CrossRef](#)]
80. Sharma, A.; Ahmad, J.; Flora, S.J.S. Application of advanced oxidation processes and toxicity assessment of transformation products. *Environ. Res.* **2018**, *167*, 223–233. [[CrossRef](#)]
81. Kim, K.H.; Kabir, E.; Jahan, S.A. Exposure to pesticides and the associated human health effects. *Sci. Total Environ.* **2017**, *575*, 525–535. [[CrossRef](#)] [[PubMed](#)]
82. Caux, P.Y.; Ménard, L.; Kent, R.A. Comparative study of the effects of MCPA, butylate, atrazine, and cyanazine on *Selenastrum capricornutum*. *Environ. Pollut.* **1996**, *92*, 219–225. [[CrossRef](#)]
83. Muñoz, M.J.; Ramos, C.; Tarazona, J.V. Bioaccumulation and toxicity of hexachlorobenzene in *Chlorella vulgaris* and *Daphnia magna*. *Aquat. Toxicol.* **1996**, *35*, 211–220. [[CrossRef](#)]
84. Chaufan, G.; Juárez, Á.; Basack, S.; Ithuralde, E.; Sabatini, S.E.; Genovese, G.; Oneto, M.; Kesten, E.; Ríos de Molina, M.D.C. Toxicity of hexachlorobenzene and its transference from microalgae (*Chlorella kessleri*) to crabs (*Chasmagnathus granulatus*). *Toxicology* **2006**, *227*, 262–270. [[CrossRef](#)]
85. Ji, J.; Long, Z.; Lin, D. Toxicity of oxide nanoparticles to the green algae *Chlorella* sp. *Chem. Eng. J.* **2011**, *170*, 525–530. [[CrossRef](#)]
86. Daghrir, R.; Drogui, P.; Robert, D. Modified TiO<sub>2</sub> for environmental photocatalytic applications: A review. *Ind. Eng. Chem. Res.* **2013**, *52*, 3581–3599. [[CrossRef](#)]
87. Ibhaddon, A.O.; Fitzpatrick, P. Heterogeneous photocatalysis: Recent advances and applications. *Catalysts* **2013**, *3*, 189–218. [[CrossRef](#)]
88. Gilja, V.; Katancic, Z.; Krehula, L.K.; Mandic, V.; Hrnjak-Murgic, Z. Efficiency of TiO<sub>2</sub> catalyst supported by modified waste fly ash during photodegradation of RR45 dye. *J. Sel. Top. Quantum Electron.* **2019**, *26*, 292–300. [[CrossRef](#)]
89. Balakrishnan, A.; Appunni, S.; Gopalram, K. Immobilized TiO<sub>2</sub>/chitosan beads for photocatalytic degradation of 2,4-dichlorophenoxyacetic acid. *Int. J. Biol. Macromol.* **2020**, *161*, 282–291. [[CrossRef](#)]
90. Bi, Q.; Huang, X.; Dong, Y.; Huang, F. Conductive Black Titania Nanomaterials for Efficient Photocatalytic Degradation of Organic Pollutants. *Catal. Lett.* **2020**, *150*, 1346–1354. [[CrossRef](#)]

91. Bockenstedt, J.; Vidwans, N.A.; Gentry, T.; Vaddiraju, S. Catalyst recovery, regeneration and reuse during large-scale disinfection of water using photocatalysis. *Water* **2021**, *13*, 2623. [[CrossRef](#)]
92. Chen, Y.H.; Wang, B.K.; Hou, W.C. Graphitic carbon nitride embedded with graphene materials towards photocatalysis of bisphenol A: The role of graphene and mediation of superoxide and singlet oxygen. *Chemosphere* **2021**, *278*, 130334. [[CrossRef](#)] [[PubMed](#)]
93. Prashanth, V.; Priyanka, K.; Remya, N. Solar photocatalytic degradation of metformin by TiO<sub>2</sub> synthesized using *Calotropis gigantea* leaf extract. *Water Sci. Technol.* **2021**, *83*, 1072–1084. [[CrossRef](#)] [[PubMed](#)]
94. Baran, N.; Gourcy, L. Sorption and mineralization of S-metolachlor and its ionic metabolites in soils and vadose zone solids: Consequences on groundwater quality in an alluvial aquifer (Ain Plain, France). *J. Contam. Hydrol.* **2013**, *154*, 20–28. [[CrossRef](#)] [[PubMed](#)]
95. Orge, C.A.; Pereira, M.F.R.; Faria, J.L. Photocatalytic ozonation of model aqueous solutions of oxalic and oxamic acids. *Appl. Catal. B* **2015**, *174–175*, 113–119. [[CrossRef](#)]
96. Rice, C.P.; McCarty, G.W.; Bialek-Kalinski, K.; Zabetakis, K.; Torrents, A.; Hapeman, C.J. Analysis of metolachlor ethane sulfonic acid (MESA) chirality in groundwater: A tool for dating groundwater movement in agricultural settings. *Sci. Total Environ.* **2016**, *560–561*, 36–43. [[CrossRef](#)] [[PubMed](#)]
97. Rui, Z.; Wu, S.; Peng, C.; Ji, H. Comparison of TiO<sub>2</sub> Degussa P25 with anatase and rutile crystalline phases for methane combustion. *Chem. Eng. J.* **2014**, *243*, 254–264. [[CrossRef](#)]
98. Tobaldi, D.M.; Pullar, R.C.; Seabra, M.P.; Labrincha, J.A. Fully quantitative X-ray characterisation of Evonik Aeroxide TiO<sub>2</sub> P25®. *Mater. Lett.* **2014**, *122*, 345–347. [[CrossRef](#)]
99. Mehrjouei, M.; Müller, S.; Möller, D. Degradation of oxalic acid in a photocatalytic ozonation system by means of Pilkington Active™ glass. *J. Photochem. Photobiol. A* **2011**, *217*, 417–424. [[CrossRef](#)]
100. Anton, F.A.; Ariz, M.; Alia, M. Ecotoxic effects of four herbicides (glyphosate, alachlor, chlortoluron and isoproturon) on the algae *Chlorella pyrenoidosa* Chick. *Sci. Total Environ.* **1993**, *134*, 845–851. [[CrossRef](#)]
101. Ma, J.; Lin, F.; Wang, S.; Xu, L. Toxicity of 21 herbicides to the green alga *Scenedesmus quadricauda*. *Bull. Environ. Contam. Toxicol.* **2003**, *71*, 594–601. [[CrossRef](#)] [[PubMed](#)]
102. Vonk, J.A.; Kraak, M.H.S. Herbicide Exposure and Toxicity to Aquatic Primary Producers. *Rev. Environ. Contam. Toxicol.* **2020**, *250*, 119–171. [[CrossRef](#)] [[PubMed](#)]
103. Lanasa, S.; Niedzwiecki, M.; Reber, K.P.; East, A.; Sivey, J.; Salice, C.J. Comparative Toxicity of Herbicide Active Ingredients, Safener Additives and Commercial Formulations to Non-Target Algae, *Raphidocelis subcapitata*. *Environ. Toxicol. Chem.* **2022**, *41*, 1466–1476. [[CrossRef](#)] [[PubMed](#)]
104. Liu, H.; Ye, W.; Zhan, X.; Liu, W. A comparative study of rac- and S-metolachlor toxicity to *Daphnia magna*. *Ecotoxicol. Environ. Saf.* **2006**, *63*, 451–455. [[CrossRef](#)] [[PubMed](#)]
105. Pérez, J.; Domingues, I.; Soares, A.M.V.M.; Loureiro, S. Growth rate of *Pseudokirchneriella subcapitata* exposed to herbicides found in surface waters in the Alqueva reservoir (Portugal): A bottom-up approach using binary mixtures. *Ecotoxicology* **2011**, *20*, 1167–1175. [[CrossRef](#)] [[PubMed](#)]
106. Fairchild, J.F.; Ruessler, D.S.; Carlson, A.R. Comparative sensitivity of five species of macrophytes and six species of algae to atrazine, metribuzin, alachlor, and metolachlor. *Environ. Toxicol. Chem.* **1998**, *17*, 1830–1834. [[CrossRef](#)]
107. Mercurio, P.; Eaglesham, G.; Parks, S.; Kenway, M.; Beltran, V.; Flores, F.; Mueller, J.; Negri, A.P. Contribution of transformation products towards the total herbicide toxicity to tropical marine organisms. *Sci. Rep.* **2018**, *8*, 4808. [[CrossRef](#)] [[PubMed](#)]
108. Sinclair, C.J.; Boxall, A.B.A. Assessing the ecotoxicity of pesticide transformation products. *Environ. Sci. Technol.* **2003**, *37*, 4617–4625. [[CrossRef](#)]
109. Osano, O.; Admiraal, W.; Klamer, H.J.C.; Pastor, D.; Bleeker, E.A.J. Comparative toxic and genotoxic effects of chloroacetanilides, formamidines and their degradation products on *Vibrio fischeri* and *Chironomus riparius*. *Environ. Pollut.* **2002**, *119*, 195–202. [[CrossRef](#)]
110. Friedman, C.L.; Lemley, A.T.; Hay, A. Degradation of chloroacetanilide herbicides by anodic Fenton treatment. *J. Agric. Food Chem.* **2006**, *54*, 2640–2651. [[CrossRef](#)]
111. Bonnet, J.L.; Bonnemoy, F.; Dusser, M.; Bohatier, J. Assessment of the potential toxicity of herbicides and their degradation products to nontarget cells using two microorganisms, the bacteria *Vibrio fischeri* and the ciliate *Tetrahymena pyriformis*. *Environ. Toxicol.* **2007**, *22*, 78–91. [[CrossRef](#)] [[PubMed](#)]
112. Virág, D.; Naár, Z.; Kiss, A. Microbial toxicity of pesticide derivatives produced with UV-photodegradation. *Bull. Environ. Contam. Toxicol.* **2007**, *79*, 356–359. [[CrossRef](#)] [[PubMed](#)]
113. Mestankova, H.; Escher, B.; Schirmer, K.; von Gunten, U.; Canonica, S. Evolution of algal toxicity during (photo)oxidative degradation of diuron. *Aquat. Toxicol.* **2011**, *101*, 466–473. [[CrossRef](#)] [[PubMed](#)]
114. Berberidou, C.; Kitsiou, V.; Karahanidou, S.; Lambropoulou, D.A.; Kouras, A.; Kosma, C.I.; Albanis, T.; Poullos, I. Photocatalytic degradation of the herbicide clopyralid: Kinetics, degradation pathways and ecotoxicity evaluation. *J. Chem. Technol. Biotechnol.* **2016**, *91*, 2510–2518. [[CrossRef](#)]
115. OECD. *Test No. 201: Freshwater Alga and Cyanobacteria, Growth Inhibition Test OECD Guidelines for the Testing of Chemicals, Section 2*; OECD Publishing: Paris, France, 2011. [[CrossRef](#)]
116. Bischoff, H.W.; Bold, H.C. Some soil algae from enchanted rock and related algae species. *Phycol. Res.* **1963**, *44*, 1–95.